

Non-Traumatic Bone Marrow Edema of the Knee: Diagnostic Accuracy of Dual-Energy Computed Tomography in Comparison to MRI

Giovanni Foti^{1,*}, Enrica Bassi¹, Luigi Romano¹, Venanzio Iacono², Gerardo Serra³, Roberto Filippini⁴ and William Mantovani⁵

¹Department of Radiology, IRCCS Sacro Cuore Don Calabria Hospital, Negrar, Italy

²Department of Orthopaedic Surgery, IRCCS Sacro Cuore Don Calabria Hospital, Negrar, Italy

³Department of Anesthesia and Analgesic Therapy, IRCCS Sacro Cuore Don Calabria Hospital, 37024 Negrar, Italy

⁴Department of Sports Medicine, IRCCS Sacro Cuore Don Calabria Hospital, Negrar, Italy

⁵Clinical and evaluative Epidemiology Unit, Public Health Trust, Trento

Abstract: *Purpose:* To evaluate the diagnostic accuracy of dual-energy computed tomography (DECT) to identify non-traumatic bone marrow edema (BME) of the knee.

Methods: This prospective study, approved by the institutional review board, comprised a cohort of 40 consecutive patients (comprising 23 males and 17 females, with a mean age of 52.3 years) who underwent examination using Dual-Energy Computed Tomography (DECT) with settings of 80 kV and a tin filter at 150 kV, in addition to Magnetic Resonance Imaging (MRI), all conducted within 5 days. Subsequently, DECT data underwent post-processing and were evaluated by two experienced radiologists, resulting in the visualization of Bone Marrow Edema (BME) on color-coded maps. To determine the diagnostic accuracy of DECT in detecting BME, receiver operator curves and the area under the curve (AUC) were computed, with MRI serving as the reference standard. Interobserver agreement was calculated with k-statistics. A p-value <0.05 was considered significant.

Results: At MRI, BME was identified in 30/40 patients, with 106/480 (22,1%) involved partitions. Sensitivity and specificity of Reader 1 were 67,9% (95% CI: 58,2 - 76,7) and 95,99% (95% CI: 93,5 - 97,7), respectively. Sensitivity and specificity of Reader 2 were 69,8% (95% CI: 60,1 - 78,3) and 95,99% (95% CI: 93,5 - 97,7), respectively. Similar diagnostic accuracy values were achieved by the 2 readers, with an AUC of 0.82 for R1 and 0.829 for R2 (p=.743). The inter-observer agreement was k=0.68.

Conclusions: DECT is an accurate imaging technique for the evidence of non-traumatic BME of the knee when compared to MRI.

Keywords: Dual energy, CT, Bone edema, Knee, MRI.

INTRODUCTION

Bone marrow edema (BME) is a significant contributor to knee pain, in both traumatic and nontraumatic patients [1-7]. Recent studies have shown that BME is prevalent in patients with knee pain, detected by magnetic resonance imaging (MRI) [8-11]. Remarkably, non-traumatic BME could be associated with conditions like osteochondral lesions (OCL), avascular necrosis, sub-chondral fractures, and transient bone marrow edema syndrome [7, 12].

The incidence of these conditions tends to increase as the population ages and the worsening of osteoarthritis. In many cases, articular space narrowing, and cartilage loss are associated with varying degrees of BME development [4, 6, 7]. Accurately assessing the presence and distribution of BME in the knee is crucial for determining the most appropriate therapeutic approach [13, 14].

MRI, particularly with fat-saturated imaging techniques, is the most reliable tool for evaluating traumatic and non-traumatic knee conditions, allowing for the assessment of ligaments, tendons, menisci, cartilage loss, and the identification of associated BME [7, 8-14]. However, an increasing number of patients cannot undergo MRI due to contraindications or the existence of metal artifacts.

*Address correspondence to this author at the IRCCS Sacro Cuore Don Calabria Hospital, Department of Radiology, Via Don A. Sempredoni 10. 37024, Negrar (VR), Italy;
Tel: 0039 0456013874;
E-mail: gfoti81@yahoo.it; Giovanni.foti@sacrocuore.it

In this context, dual-energy computed tomography (DECT) emerges as a valuable alternative for evaluating patients with painful knees unable to undergo MRI. DECT has the advantages of conventional CT imaging, offering isotropic high-resolution images with bone window, a large gantry, rapid scanning, and minimal motion artifacts, all without the issues of claustrophobia. Furthermore, the introduction of virtual non-calcium imaging techniques (VNCa) has enabled the successful identification of knee BME [15-22].

In particular, a systematic meta-analysis evaluated the diagnostic accuracy of DECT for detecting BME in adult patients with acute knee injuries [22]. The reported sensitivity, specificity, and AUROC values for BME were 84%, 96%, and 0.97, respectively [22].

However, the majority of papers focused on traumatic BME, in acute or sub-acute phases [15-22]. The detection of knee BME in non-traumatic conditions [12], particularly in the presence of osteoarthritis, presents a significant advantage when MRI is unavailable or contraindicated. Additionally, DECT could offer the benefit of detecting associated imaging findings, as demonstrated in studies focusing on the ankle and hip [23-25].

Therefore, the purpose of this study was to evaluate the diagnostic accuracy of DECT in the identification of non-traumatic BME of the knee, using MRI as the standard of reference.

MATERIAL AND METHODS

Patient Population

This prospective research received the Institutional Review Board approval and informed consent was obtained from all participating patients. In the period between January 2022 to September 2023, 51 consecutive patients were considered for inclusion.

Patients were referred to the radiology department following an orthopedic visit. Inclusion criteria consisted of the presence of knee pain, absence of recent trauma (within 6 months), and negative conventional radiographs. All patients underwent MRI and DECT within 5 days. Exclusion criteria were absence of imaging studies, previous surgery, and oncologic disease.

From a clinical point of view, DECT scans were utilized to evaluate the bone anatomical aspects of the knee and the presence of calcifications, while MRI

results were employed to assess the presence of bone marrow edema (BME) and to examine the condition of knee ligaments and tendons.

DECT Protocol

Dual-energy computed tomography (DECT) scans were conducted using a 384-slice dual-source CT scanner (Somatom® Definition Force, Siemens Healthcare, Forchheim, Germany). The scanning parameters were configured as follows: tube A operated at 80 kV, while tube B operated at 150 kV, with the inclusion of a tin filter for enhancement. The preset tube current-time product was established at a precise ratio of 1.6:1, which translated to 220 quality reference mAs for tube A and 138 quality reference mAs for tube B. To ensure optimal radiation dose management, we implemented automated attenuation-based tube current modulation, utilizing CARE dose 4D technology developed by Siemens Healthcare. In terms of radiation exposure, the mean effective post-scan volume CT dose index was calculated at 8.8 Gy (range 5.9 to 11.8 mGy). Similarly, the dose-length product was computed at 134.6 mGy/cm (range 83.2 to 179.4 mGy-cm). These dose parameters were found to be consistent with our established standard CT protocol for knee examinations, ensuring the reliability and comparability of our imaging practices.

DECT Post-Processing

The 80-kVp dataset and the 150-kVp dataset with a tin filter with soft-tissue kernel (Qr32) were reconstructed on a dedicated offline workstation (SyngoVia® VB20) by using Virtual Non-Calcium (VNCa) application. The resulting color-coded maps specific to dual-energy imaging were integrated with conventional gray-scale morphological images (slice thickness of 1 mm and an increment of 1 mm).

MRI Protocol

Magnetic resonance imaging (MRI) was conducted utilizing a commercially available 1.5-Tesla MRI system (Magnetom Avanto Fit; Siemens Healthcare, Erlangen, Germany). The imaging protocol encompassed standard sequences, including 4-mm thick T1-weighted turbo spin-echo sequences (with parameters TR/TE/FA = 650.0 ms/18.0 ms/150°) and T2-weighted turbo spin-echo sequences (with parameters TR/TE = 4300.0 ms/124.0 ms), administered both in axial and coronal orientations. Additionally, turbo inversion recovery magnitude (TIRM) sequences, characterized by a

TR/TE of 3500.0 ms/39.0 ms, were acquired exclusively in the coronal plane to further augment the imaging dataset.

Image Analysis

In both MRI and DECT images, the diagnosis of bone marrow edema (BME) was established using a binary classification system, with "1" signifying the presence of BME and "0" denoting its absence. To enhance the precision of BME assessment, the lower femur and upper tibia regions were subdivided into six discrete segments, as done in a similar previous study [12]. Therefore, for each patient, 12 partitions were available for analysis. As the reference standard for assessment of BME, all MRI images were reviewed by two experienced radiologists (22 and 14 years of experience), in consensus, unaware of clinical and CT findings. At MRI, the diagnosis of BME was based on the presence of signal hyperintensity on TIRM images and hypointense signals on T1-weighted imaging.

Subsequently, in a separate reading session, DECT images were reviewed by two different independent radiologists (12 and 5 years of experience), in a random order, blinded to clinical and MRI findings.

At DECT, the diagnosis of Bone Marrow Edema (BME) relied on identifying regions of heightened bone density, which corresponded to elevated water content as depicted by shades ranging from green to yellow on the DECT map. This comparison was made in relation to adjacent unaffected bone tissue.

Each reader was free to choose his preferred settings for visualizing reconstructed images. In particular, regarding the default settings for color-coded maps, density ranges were established between -150 and 100 Hounsfield Units (HU), with color-coded maps superimposed exclusively when density values exceeded the -50 HU threshold. In adherence to these default settings, normal bone, characterized by density values below -50 HU, appeared without any color superimposition. The diagnosis of BME was predicated on the presence of superimposed colors, ranging from violet-blue (indicating mild edema) to green-yellow or orange-red (indicating severe edema). The presence of shades of green on 3D maps confirmed the presence of BME.

Additionally, readers had the autonomy to adjust parameters related to the visualization of color-coded maps, including the widely adopted approach in which

BME is represented in green and normal bone is depicted in violet.

Potential contributing factors to BME, such as osteochondral lesions (OCLs), stress insufficiency, or sub-chondral fractures, were documented.

In case of discrepancies, a consensus reading was conducted, and the collectively agreed-upon results were utilized for further analysis. To assess intra-observer agreement, the DECT images were re-evaluated randomly after a 60-day interval.

Quantitative analysis of DECT data was not conducted.

STATISTICAL ANALYSIS

Continuous variables were summarized using the mean and range, spanning from the minimum to the maximum values. Categorical variables were presented in terms of numerical counts and percentages. Data underwent analysis utilizing the receiver operating characteristic (ROC) method; each reader's performance in depicting BME was evaluated for DECT reading sessions, using MRI as the reference standard. The area under the receiver operating characteristic curve (AUC) and 95% confidence intervals (CIs) were calculated. AUC was evaluated using the method of Delong *et al.* To compare the areas under two or more correlated receiver operating characteristic curves a nonparametric approach was used. The sensitivity, specificity, positive predictive values (PPV), and negative predictive values (NPV) were calculated on 480 partitions among the 40 enrolled patients. A value of p less or equal to 0.05 was considered statistically significant. Inter-observer agreement was calculated using kappa statistics.

RESULTS

A total of 40 patients participated in this study, with a median age of 52.3 years. This group comprised 23 males, with an average age of 53.5 years (ranging from 33 to 76), and 17 females, whose mean age was 51.1 years (ranging from 36 to 74).

11 patients were excluded from the study due to various reasons, including claustrophobia ($n=4$), artifacts on MRI ($n=2$), presence of pacemakers ($n=2$), oncologic disease ($n=1$), and previous surgery ($n=2$).

The diagram in Figure 1 illustrates the workflow of patients enrolled in the study.

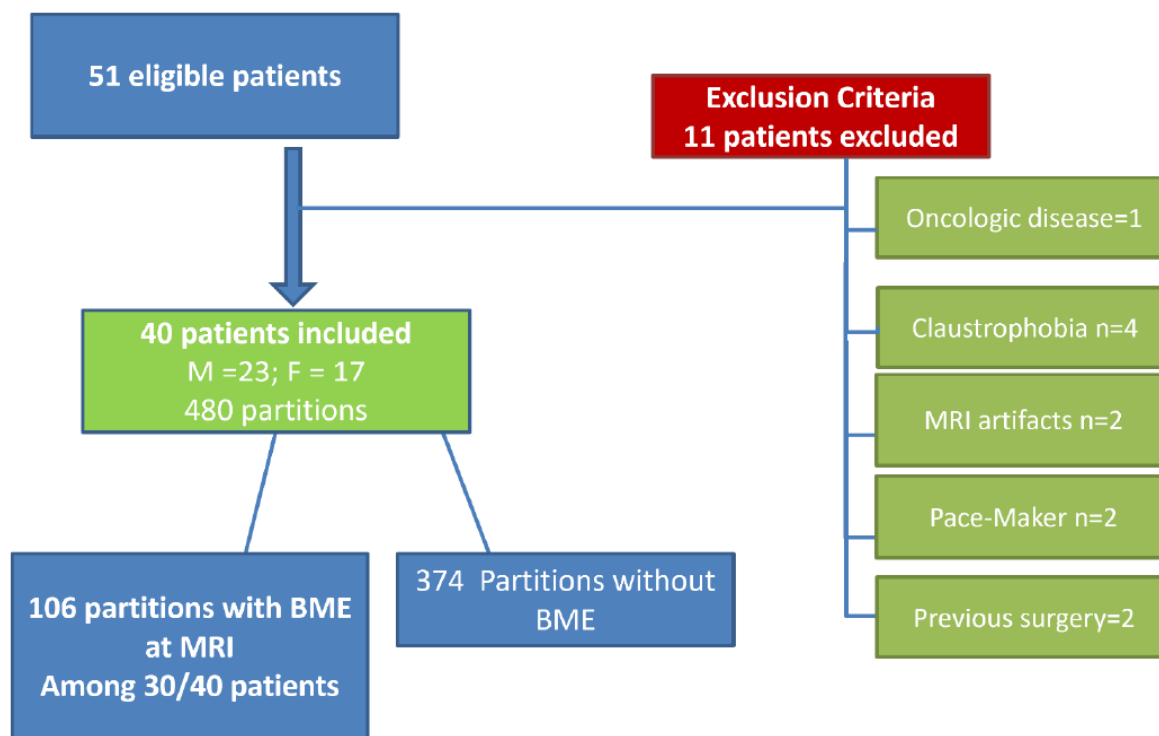


Figure 1: Workflow of patients enrolled in the study.

Clinical data about the enrolled patients are summarized in Table 1.

At MRI, BME was identified in 30/40 patients (75%), with 106/480 (22,1%) involved partitions, whereas absence of edema was reported in 374 (77,9%) cases. Among patients with BME at MRI, the clinical radiological diagnoses included stress fractures in 5 cases and osteochondral lesions in 8 cases.

The diagnostic accuracy results for DECT, on a per-partition basis, are presented in Tables 2 and 3, respectively.

Reader 1 (R1) pointed out the presence of BME at DECT in 87 (Figures 2 and 3), and its absence in 393 partitions, respectively, with Sensitivity of 67,9% (95% CI: 58,2 - 76,7), Specificity 95,99% (95% CI: 93,5 - 97,7), positive predictive values 82.8% (95% CI: 73,2 - 90), negative predictive values 91.3% (95% CI: 88,1 - 93.9).

Reader 2 (R2) pointed out the presence of BME at DECT in 89, and its absence in 391 partitions, respectively, with Sensitivity of 69,8% (95% CI: 60,1 - 78,3), Specificity 95,99% (95% CI: 93,5 - 97,7), positive predictive values 83.1% (95% CI: 73.7 - 90.2),

Table 1: Clinical Data of Patients Enrolled

Patient Population	N=40	
AGE – MEDIAN	52	(43;52)
SEX		
M	23	67.5%
F	17	42.5%
BME MRI	30	75%
CONCOMITANT LESIONS		
NO	27	67.5%
Stress Fractures	5	12.5%
Osteo-Chondral Lesions	8	20.0%

Table 2: Diagnostic Accuracy Parameters of the 2 Readers. 95% C.I = Confidence Interval; + LR = Positive Likelihood Ratio; - LR = Negative Likelihood Ratio; PPV = Positive Predictive Value; NPV = Negative Predictive Value

Parameters	Sensitivity	95% C.I.	Specificity	95% C.I.	+ LR	-LR	PPV	95% C.I.	NPV	95% C.I.
READER 1	67.9	58.2-76.7	95.99	93.5-97.7	16.94	0.33	82.8	73.2-90.0	91.3	88.1-93.9
READER 2	69.8	60.1-78.3	95.99	93.5-97.7	17.41	0.31	83.1	73.7-90.2	91.8	88.6-94.3

Table 3: Correct Classification Rate of the 2 Readers

Patient Population n=40	Total Partitions n=480
<p>DECT reader 1</p> <p>TRUE NEGATIVE 7 TRUE POSITIVE 25 FALSE NEGATIVE 5 FALSE POSITIVE 3 Correct classification rate 80 % (32/40)</p>	<p>DECT reader 1</p> <p>TRUE NEGATIVE 359 TRUE POSITIVE 72 FALSE NEGATIVE 34 FALSE POSITIVE 15 Correct classification rate 89,8% (431/480)</p>
<p>DECT reader 2</p> <p>TRUE NEGATIVE 7 TRUE POSITIVE 24 FALSE NEGATIVE 6 FALSE POSITIVE 3 Correct classification rate 77,5 % (31/40)</p>	<p>DECT reader 2</p> <p>TRUE NEGATIVE 359 TRUE POSITIVE 74 FALSE NEGATIVE 32 FALSE POSITIVE 15 Correct classification rate 90,2 % (433/480)</p>

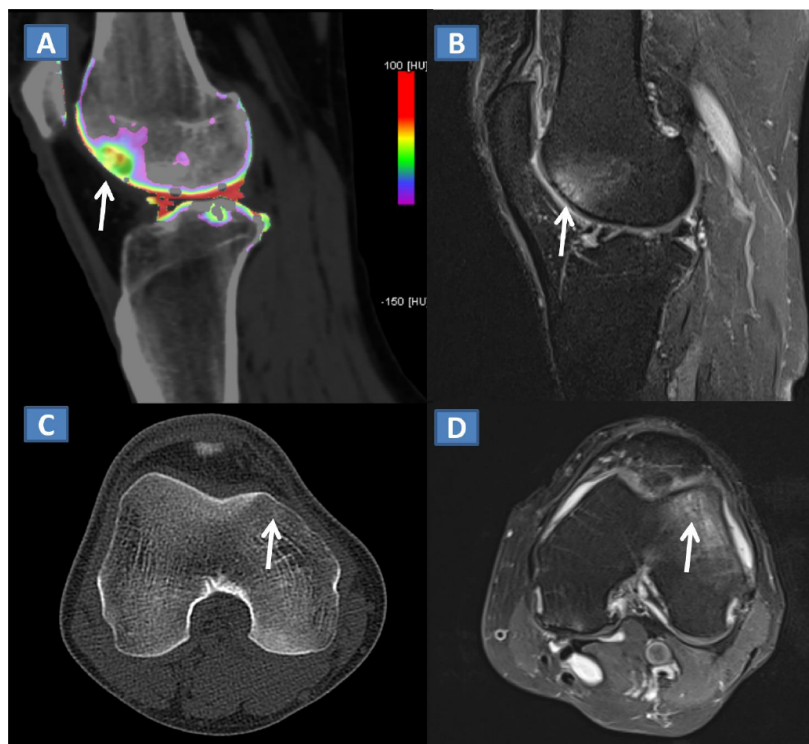


Figure 2: Sixty-one-year-old man with non-traumatic knee pain. On the sagittal DECT reconstructed 1-mm super-imposed 2D DECT color-coded image (a), BME (arrow) is coded in the shade of green-to-yellow on the lateral femoral condyle. Normal spared bone is coded without any superimposition. The presence of BME is confirmed on the corresponding sagittal (b) and axial (d) TIRM MRI images of the knee (arrow). On axial 1 mm corresponding CT image with bone window (c), there is no evidence of associated findings (arrow).

negative predictive values 91.8% (95% CI: 88,6 – 94.3).

The inter-observer agreement regarding the diagnosis of BME at DECT was k=0.68.

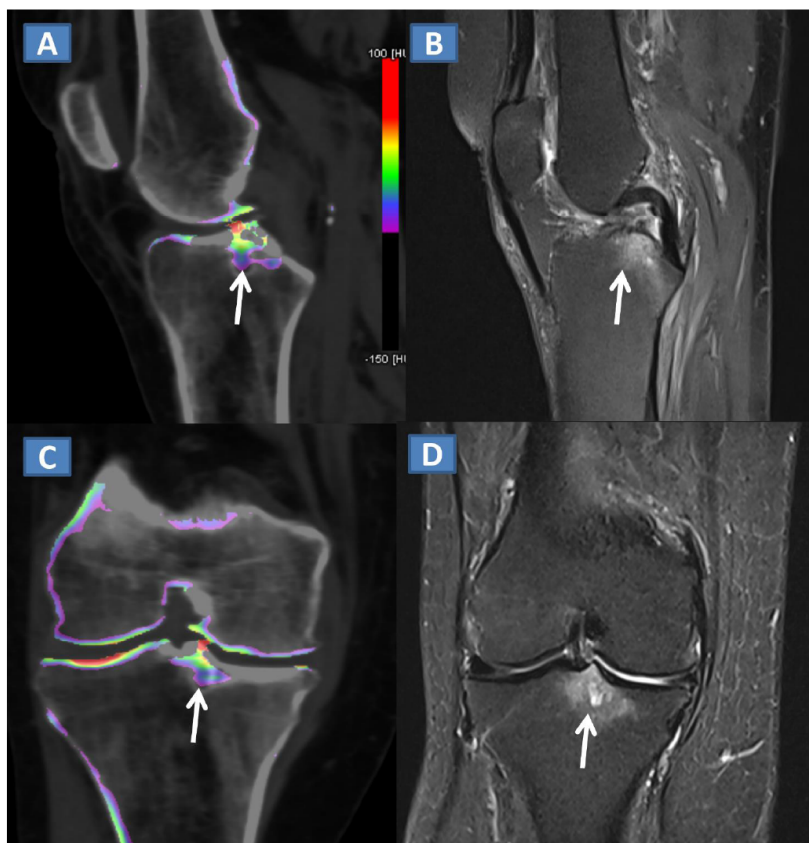


Figure 3: Seventy-two-year-old female with non-traumatic knee pain. On the sagittal (a) and coronal (c) DECT reconstructed 1-mm super-imposed 2D DECT color-coded images, BME (arrow) is coded in the shade of green-to-violet on the media tibial plateau. Normal spared bone is coded without any superimposition. The presence of BME is confirmed on the corresponding sagittal (b) and coronal (d) TIRM MRI images of the knee (arrow).

Similar diagnostic accuracy values were achieved by the 2 readers, with an AUC of 0.82 for R1 and 0.829 for R2 ($p=.743$) (Figure 4).

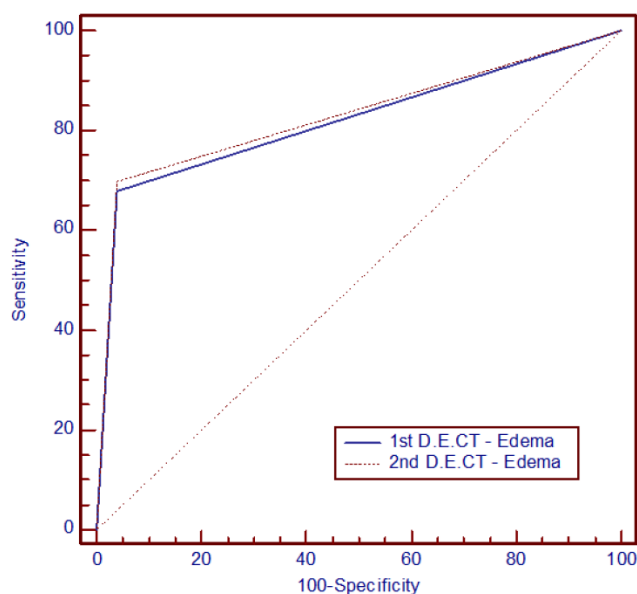


Figure 4: Comparison of AUC of Reader 1 and Reader 2 in depicting BME of the knee.

Interestingly, BME was correctly identified at DECT in 12/13 patients presenting associated findings by both readers.

DISCUSSION

In this study, we assessed the diagnostic accuracy of DECT in the evaluation of non-traumatic BME of the knee. By performing a per-partitions analysis, a strict MRI-DECT correlation was attempted as concerns the identification of BME foci in the distal femur and proximal tibia.

Our data confirmed that DECT represents a reliable imaging tool for the assessment of BME around the knee joint, with an AUC of 0.82 for R1 and 0.829 for R2 ($p=.743$) and with good inter-observer agreement ($k=0.68$).

Nonetheless, sensitivity values were inferior to those reported in previous studies, whereas specificity values were similar to those previously reported. In particular, in the paper by Booz *et al.* [19], enrolling 57 patients, 94% sensitivity and 95% specificity were

reported, respectively [19]. However, the said paper focused on traumatic knee injuries, evaluated in the acute phase. Also, the mean age of patients enrolled was inferior as compared to that of our study population. Similarly, Wang *et al.* [20], by performing a quantitative evaluation of BME in the knee, obtained a sensitivity and specificity of 88.4 and 98% for DECT, respectively. Once again, the authors enrolled traumatic patients only. Differently from the above-mentioned study, as done in some recently published papers [26, 27], we focused on qualitative assessment of BME. Our choice was based on possible variations of DECT numbers around the knee joint, due to the presence of complex anatomy, with thick cortical bone near the articular cavity or bone sclerosis, that can generate both false negative and false positive findings. By locally increasing bone density, peri-articular bone sclerosis can affect the measurement of DECT density as well. In our experience, this problem is more commonly encountered in aged patients, often associated with knee osteoarthritis.

A recent metanalysis focusing on the detection of non-traumatic BME by DECT included ten studies involving 2463 regions (hands, ankles, hips, and sacroiliac joints) [28]. Summary sensitivity, specificity, and area under the receiver operating characteristic curve values for BME detection were 88.4%, 96.1%, and 0.98, respectively. However, there are no papers available concerning non-traumatic BME of the knee. In a previous study enrolling a mixed traumatic and non-traumatic cohort [12], the sensitivity and specificity of per-partition analysis were 92.9 and 92.9 for reader 1, and 88.2 and 93.9 for reader 2 [12]. Nevertheless, all patients with traumatic BME were correctly diagnosed by both readers, whereas non-traumatic BME was missed in 2 patients by reader 1 and in 3 patients by reader 2, respectively [12].

Conversely, our specificity values were relatively high, and in line with previous studies. A Possible explanation is the choice to perform a partition analysis, which allowed us to have many spared partitions for each patient, with a subsequent increase of specificity. Conversely, we had relatively few false positive cases due to bone sclerosis.

Among the 30 patients suffering from BME, 15 (50%) presented an associated imaging finding, including OCL or stress or sub-chondral fractures. These findings are usually well depicted on standard CT images alone and are often associated with severe BME. Although we did not grade BME at MRI and

DECT, we presume that severe BME should be much more easily depicted at DECT concerning mild BME.

Our results suggest that diagnosing BME in non-traumatic patients could be more difficult than in traumatic ones. However, there are no papers focusing on the comparison between mild versus severe non-traumatic BME depiction by DECT so far [28].

According to our results, DECT could represent an alternative imaging tool for the identification and follow-up of non-traumatic BME of the knee, especially in aged patients and in case of severe edema with associated imaging findings. With aging of the population indeed, the possibility of having some MRI contraindication increase, whereas the problem of radiation exposure come less. The mean post-scan CTDI vol in our study was similar to those of similar previous studies.

This study has some limitations. First, we enrolled a relatively limited number of patients. A larger cohort would be required to validate our results. Also, only qualitative analysis of BME was performed. However, this choice is partially related to the need to perform a partitions analysis, which allowed us to compensate the relatively limited study population. Further to this, a sub-analysis of associated imaging findings, or a comparison of elderly versus young patients was not performed because of the relatively limited numbers.

The integration of artificial intelligence and deep learning systems are increasingly being employed within the field of musculoskeletal radiology, with application both in dual energy TC and MRI studies [e.g. 29; 30; 31]. Especially, Park *et al.* have shown the remarkable proficiency of artificial intelligence systems in detecting hip bone marrow edema in dual-energy CT studies, surpassing the capabilities of less experienced radiologists [31]. In the future therefore, detection of edema by dual energy CT could be even more accurate and objective with the use of deep learning and AI software.

In conclusion, DECT showed high overall diagnostic accuracy in depicting non-traumatic BME of the knee and could be considered as an alternative imaging tool for the assessment of knee pain when MRI is not available.

DISCLOSURE

The authors declare that they have no conflict of interest.

ETHICAL APPROVAL

All procedures performed in studies involving human participants were in accordance with the ethical standard of the institutional and/or national research committee and with the 1964 Helsinki declaration and its later amendments or comparable ethical standard.

Informed consent was obtained by all patients enrolled for this retrospective study.

FOUND INFORMATION

We did not receive any funds for this paper.

REFERENCES

- [1] Molfetta L, Florian A, Saviola G, Frediani B. Bone Marrow Edema: pathogenetic features. *Clin Ter.* 2022 Sep-Oct; 173(5): 434-439.
- [2] Pearl MC, Mont MA, Scuderi GR. Osteonecrosis of the Knee: Not all Bone Edema is the Same. *Orthop Clin North Am.* 2022 Oct; 53(4): 377-392. <https://doi.org/10.1016/j.ocl.2022.06.002>
- [3] Kon E, Ronga M, Filardo G, Farr J, Madry H, Milano G, Andriolo L, Shabshin N. Bone marrow lesions and subchondral bone pathology of the knee. *Knee Surg Sports Traumatol Arthrosc.* 2016 Jun; 24(6): 1797-814. <https://doi.org/10.1007/s00167-016-4113-2>
- [4] Zhang HJ, Ye SY, Wang XJ, Tong PJ. [Research progress of bone marrow edema-like lesions in knee osteoarthritis]. *Zhongguo Gu Shang.* 2021 Dec 25; 34(12): 1186-90. Chinese.
- [5] Manara M, Varenna M. A clinical overview of bone marrow edema. *Reumatismo.* 2014 Jul 28; 66(2): 184-96. <https://doi.org/10.4081/reumatismo.2014.790>
- [6] Collins JA, Beutel BG, Strauss E, Youm T, Jazrawi L. Bone Marrow Edema: Chronic Bone Marrow Lesions of the Knee and the Association with Osteoarthritis. *Bull Hosp Jt Dis (2013).* 2016 Mar; 74(1): 24-36. PMID: 26977546.
- [7] Gorbachova T, Melenevsky Y, Cohen M, Cerniglia BW. Osteochondral Lesions of the Knee: Differentiating the Most Common Entities at MRI. *Radiographics.* 2018 Sep-Oct; 38(5): 1478-1495. <https://doi.org/10.1148/rq.2018180044>
- [8] Berger CE, Kröner AH, Kristen KH, *et al* (2006) Transient bone marrow edema syndrome of the knee: clinical and magnetic resonance imaging results at 5 years after core decompression. *Arthroscopy* 22: 866-871 8. <https://doi.org/10.1016/j.arthro.2006.04.095>
- [9] Lecouvet FE, van de Berg BC, Maldague BE, *et al* (1998) Early irreversible osteonecrosis versus transient lesions of the femoral condyles: prognostic value of subchondral bone and marrow changes on MR imaging. *AJR Am J Roentgenol* 170(1): 71-77 9. <https://doi.org/10.2214/ajr.170.1.9423603>
- [10] Carey JL, Shea KG (2016) AAOS appropriate use criteria: management of osteochondritis dissecans of the femoral condyle. *J Am Acad Orthop Surg* 24(9): e105-e111 10. <https://doi.org/10.5435/JAAOS-D-16-00227>
- [11] Berkem L, Turkmen I, Unay K, Akcal MA, Aydemir N (2013) Factors influencing outcome of knee bone marrow edema: a clinical study. *Acta Orthop Belg* 79(5): 572-577
- [12] Foti G, Mantovani W, Faccioli N, Crivellari G, Romano L, Zorzi C, Carbogin G. Identification of bone marrow edema of the knee: diagnostic accuracy of dual-energy CT in comparison with MRI. *Radiol Med.* 2021 Mar; 126(3): 405-41. <https://doi.org/10.1007/s11547-020-01267-y>
- [13] Hofmann S, Kramer J, Breitenseher M *et al* (2006) Bone marrow edema in the knee. Differential diagnosis and therapeutic possibilities. *Orthopade* 35: 463-475 4.
- [14] Zanetti M, Bruder E, Romero J, *et al* (2000) Bone marrow edema pattern in osteoarthritic knees: correlation between MR imaging and histologic findings. *Radiology* 215: 835-840 <https://doi.org/10.1148/radiology.215.3.r00j05835>
- [15] Cao JX, Wang YM, Kong XQ, Yang C, Wang P (2015) Good interrater reliability of a new grading system in detecting traumatic bone marrow lesions in the knee by dual-energy CT virtual non-calcium images. *Eur J Radiol* 84(6): 1109-1115. <https://doi.org/10.1016/j.ejrad.2015.03.003>
- [16] Suh CH, Yun SJ, Jin W *et al.* (2018) Diagnostic performance of dual-energy CT for the detection of bone marrow edema: a systematic review and meta-analysis. *Eur Radiol* 28(10): 4182-4194. <https://doi.org/10.1007/s00330-018-5411-5>
- [17] Ai S, Qu M, Glazebrook KN, *et al* (2014) Use of dual-energy CT and virtual non-calcium techniques to evaluate post-traumatic bone bruises in knees in the subacute setting. *Skeletal Radiol* 43: 1289-1295 <https://doi.org/10.1007/s00256-014-1913-7>
- [18] Pache G, Bulla S, Baumann T *et al.* (2012) Dose reduction does not affect detection of bone marrow lesions with dual-energy CT virtual noncalcium technique. *Acad Radiol* 19(12): 1539-1545 <https://doi.org/10.1016/j.acra.2012.08.006>
- [19] Booz C, Nöske J, Lenga L, Martin SS, Yel I, Eichler K, *et al.* (2019) Color-coded virtual non-calcium dual-energy CT for the depiction of bone marrow edema in patients with acute knee trauma: a multi-reader diagnostic accuracy study. *Eur Radiol.* <https://doi.org/10.1007/s00330-019-06304-7>
- [20] Wang MY, Zhang XY, Xu L, Feng Y, Xu YC, Qi L, Zou YF (2019) Detection of bone marrow edema in knee joints using a dual-energy CT virtual non-calcium technique. *Clin Radiol* 74(10): 815.e1-815.e7. <https://doi.org/10.1016/j.crad.2019.06.020>
- [21] Björkman AS, Koskinen SK, Lindblom M, Persson A (2019) Diagnostic accuracy of dual-energy CT for detection of bone marrow lesions in the subacutely injured knee with MRI as reference method. *Acta Radiol* 3: 284185119877343. <https://doi.org/10.1177/0284185119877343>
- [22] Wilson MP, Lui K, Nobbie D, Murad MH, Katlariwala P, Low G. Diagnostic accuracy of dual-energy CT for detecting bone marrow edema in patients with acute knee injuries: a systematic review and meta-analysis. *Skeletal Radiol.* 2021 May; 50(5): 871-879. <https://doi.org/10.1007/s00256-020-03646-y>
- [23] Foti G, Serra G, Iacono V, Marocco S, Bertoli G, Gori S, Zorzi C. Identification of Non-Traumatic Bone Marrow Oedema: The Pearls and Pitfalls of Dual-Energy CT (DECT). *Tomography.* 2021 Aug 26; 7(3): 387-396. <https://doi.org/10.3390/tomography7030034>
- [24] Foti G, Guerriero M, Faccioli N, Figuera A, Romano L, Zorzi C, Carbogin G. Identification of bone marrow edema around the ankle joint in non-traumatic patients: Diagnostic accuracy of dual-energy computed tomography. *Clin Imaging.* 2021 Jan; 69: 341-348. <https://doi.org/10.1016/j.clinimag.2020.09.013>
- [25] Foti G, Faccioli N, Silva R, Oliboni E, Zorzi C, Carbogin G. Bone marrow edema around the hip in non-traumatic pain: dual-energy CT vs MRI. *Eur Radiol.* 2020 Jul; 30(7): 4098-4106. <https://doi.org/10.1007/s00330-020-06775-z>
- [26] Ghazi Sherbaf F, Sair HI, Shakoor D, Fritz J, Schwaiger BJ, Johnson MH, Demehri S. DECT in Detection of Vertebral Fracture-associated Bone Marrow Edema: A Systematic Review and Meta-Analysis with Emphasis on Technical and Imaging Interpretation Parameters. *Radiology.* 2021 Jul;

- 300(1): 110-119.
<https://doi.org/10.1148/radiol.2021203624>
- [27] Suh CH, Yun SJ, Jin W, Lee SH, Park SY, Ryu CW. Diagnostic performance of dual-energy Radiol. 2018 Oct; 28(10): 4182-4194.
<https://doi.org/10.1007/s00330-018-5411-5>
- [28] Chen Z, Chen Y, Zhang H, Jia X, Zheng X, Zuo T. Diagnostic accuracy of dual-energy computed tomography (DECT) to detect non-traumatic bone marrow edema: A systematic review and meta-analysis. Eur J Radiol. 2022 Aug; 153: 110359.
<https://doi.org/10.1016/j.ejrad.2022.110359>
- [29] Astuto B, Flament I, K. Namiri N, Shah R, Bharadwaj U, M. Link T, & Majumdar S. Automatic deep learning-assisted detection and grading of abnormalities in knee MRI studies. Radiology: Artificial Intelligence, 2021; 3(3): e200165.
<https://doi.org/10.1148/ryai.2021200165>
- [30] Calivà F, Namiri NK, Dubreuil M, Pedoia V, Ozhinsky E, & Majumdar S. Studying osteoarthritis with artificial intelligence applied to magnetic resonance imaging. Nature Reviews Rheumatology, 2022; 18(2): 112-121.
<https://doi.org/10.1038/s41584-021-00719-7>
- [31] Park C, Kim M, Park C, Son W, Lee SM, Jeong HS, & Choi MH. Diagnostic performance for detecting bone marrow edema of the hip on dual-energy CT: Deep learning model vs. musculoskeletal physicians and radiologists. European Journal of Radiology, 2022; 152: 110337.
<https://doi.org/10.1016/j.ejrad.2022.110337>

Received on 03-09-2023

Accepted on 05-10-2023

Published on 11-10-2023

DOI: <https://doi.org/10.12974/2313-0954.2023.09.03>

© 2023 Foti *et al.*

This is an open access article licensed under the terms of the Creative Commons Attribution Non-Commercial License (<http://creativecommons.org/licenses/by-nc/3.0/>) which permits unrestricted, non-commercial use, distribution and reproduction in any medium, provided the work is properly cited.